

NMR evidence for formation of octahedral and tetrahedral Al and repolymerization of the Si network during dissolution of aluminosilicate glass and crystal

NATIA TSOMAIA,^{1,*} SUSAN L. BRANTLEY,² JAMES P. HAMILTON,^{3,†} CARLO G. PANTANO,³ AND KARL T. MUELLER^{1,‡}

¹Department of Chemistry and Materials Research Institute, Penn State University, University Park, Pennsylvania 16802, U.S.A.

²Department of Geosciences and Materials Research Institute, Penn State University, University Park, Pennsylvania 16802, U.S.A.

³Department of Materials Science and Engineering, and Materials Research Institute, Penn State University, University Park, Pennsylvania 16802, U.S.A.

ABSTRACT

Five sodium aluminosilicate glasses in the series $\text{Na}_2\text{O} : x\text{Al}_2\text{O}_3 : (3-x)\text{SiO}_2$ and $\text{Na}_2\text{O} : \text{Al}_2\text{O}_3 : y\text{SiO}_2$ were prepared and subjected to leaching at pH 2 under ambient conditions for up to 1000 h. Solid-state nuclear magnetic resonance (NMR) spectroscopy revealed the identity of aluminate and silicate environments in the leached surface layers of these glasses as well as a sample of albite crystal subjected to the same aqueous leaching. While ^{29}Si and ^{27}Al magic-angle spinning (MAS) NMR experiments report on the bulk structures of the samples, cross-polarization from hydrogen atoms that are present only in the surface layers provides structural information from the regions of the sample transformed during treatment. Aluminum in octahedral coordination by O atoms (Al^{VI}) is confirmed for the first time on the near-surface region of an albite crystal under the treatment conditions of this study. A quantification of the change in the amount of six-coordinate aluminum as a function of bulk Al/Si ratio is made possible by comparing the relative amounts of $^1\text{H} \rightarrow ^{27}\text{Al}$ CPMAS signals from Al^{IV} and Al^{VI} obtained from different samples under reproducible experimental conditions. The relative contribution of Al^{VI} to total Al in the hydrated layers increases with the Al/Si ratio of the glasses studied. The leached albite crystal sample has an anomalously high concentration of Al^{VI} given its Al/Si ratio. This anomaly is probably related to the relatively low thickness of the leached layer developed on this phase: little hydrogen penetrates the crystal surface and almost all of the Al in the thin leached layer is octahedrally coordinated, similar to Al in solution. These data suggest that hydrolysis of bridging O atoms around Al atoms in the glass or crystal hydrated layer is accompanied by a change in the coordination number of the Al atom. Aging of surfaces documents no formation of Al^{VI} during storage after leaching. The MAS data, coupled with $^{27}\text{Al} \rightarrow ^{29}\text{Si}$ CPMAS experiments, describe the bulk network structure and provide further insight into the surface structures, including documentation of repolymerization of the silicon network in the surface layer of a nepheline glass via formation of condensed Q^4 units. Further triple-resonance experiments correlate ^1H , ^{29}Si , and ^{27}Al environments in the glasses, and indicate that the repolymerized structures in nepheline glass are not phase-separated from aluminum-containing network structures. These data for acid dissolution under ambient conditions yield the first picture of the complicated series of reactions relating connectivity and coordination number of Al and Si at the altered surfaces of geologically interesting aluminosilicates.

INTRODUCTION

The mechanisms of dissolution of feldspar, the most common mineral in the crust, is still not understood despite intense analysis (e.g., Casey et al. 1988a; Brady and Walther 1989; Casey et al. 1989; Hellmann et al. 1990; Blum and Lasaga 1991; Oelkers et al. 1994; Blum and Stillings 1995; Oelkers and Schott 1995; Brantley and Stillings 1996; Walther 1996; Brantley and

Stillings 1997; Hellmann et al. 1997; Walther 1997). Understanding the mechanisms is complicated by the fact that dissolution has been reported to be initially nonstoichiometric for most sub-neutral conditions of pH. Initial dissolution may or may not be stoichiometric under near neutral pH conditions, where dissolution data at steady state is sparse. Under acid conditions, the charge-balancing cation (Na^+ , K^+ , or Ca^{2+}) and Al are removed preferentially until the surface develops a Si-enriched layer that eventually dissolves stoichiometrically (e.g., Stillings and Brantley 1995). Because the surface chemistry of dissolving feldspar is not stoichiometric in most solutions, a steady state surface chemistry is inferred to control dissolution. An enhanced and more complete understanding of such steady state surface conformations will produce better models for feldspar dissolution.

* Current address: Department of Molecular Pharmacology, Physiology, and Biotechnology, Brown University, Providence, Rhode Island 02912. Natia_Tsomaia@Brown.edu

† Current address: Johns Manville Inc. 10100 West Ute Ave. Littleton, Colorado 80127. E-mail: HamiltonJ@JM.com

‡ E-mail: ktm2@psu.edu

Due to the coordination change between Al in feldspar (four-fold) and Al in solution (sixfold), it has been suggested that surface Al might be present on the dissolving feldspar surface in varying coordinations (e.g., Casey and Bunker 1990; Hellmann 1995). Several workers have also suggested that the silica network of feldspar repolymerizes during dissolution under acid conditions (Casey and Bunker 1990; Hellmann et al. 1990; Stillings and Brantley 1995). In order to investigate the coordination of Al and Si on the surface of dissolving feldspar, we treated glassy and crystalline powders of albite ($\text{NaAlSi}_3\text{O}_8$) composition with acidic solutions (pH = 2) at 25 °C for 1000 hours. We further synthesized and leached two series of glasses with a range of Al/Si ratios and either constant or variable Na_2O concentration to investigate the effect of Al/Si ratio on dissolution of aluminosilicates. Hamilton et al. (2000, 2001) have shown that dissolution of glasses can be used to elucidate rates and mechanisms of dissolution of feldspars of similar composition. Figure 1 presents an overview of the two suites of samples prepared and studied (the "NBO" and "mineral" glasses). Glasses with constant sodium concentration contain non-bridging O (NBO) sites in the bulk structure and lie in the join $\text{Na}_2\text{O}-x\text{Al}_2\text{O}_3-(3-x)\text{SiO}_2$ (where x equals the Al/Na ratio). For glasses with fully polymerized networks ($\text{Na}_2\text{O}-\text{Al}_2\text{O}_3-y\text{SiO}_2$), but with variable Na concentration, silica is systematically added while maintaining a constant $\text{Na}_2\text{O}/\text{Al}_2\text{O}_3$ ratio of 1; these glasses are analogues of the aluminosilicate minerals albite, jadeite, and nepheline, and therefore they are referred to as the "mineral glasses." Spectrochemical characterization of all glass samples prepared for this study is given in Table 1. At a pH of 2, the dissolution rates of the two suites of glasses, listed in Table 2, increase with increasing bulk Al/Si ratio (Hamilton 1999; Hamilton et al. 2001); however, for the same Al/Si ratio, the rate of dissolution also increases with the average number of NBO sites per silicate tetrahedral unit (see Fig. 2).

Altered layers formed on these glass surfaces leached at pH = 2 have been previously investigated (Hamilton and Pantano 1997; Hamilton et al. 2000; Hamilton et al. 2001). X-ray pho-

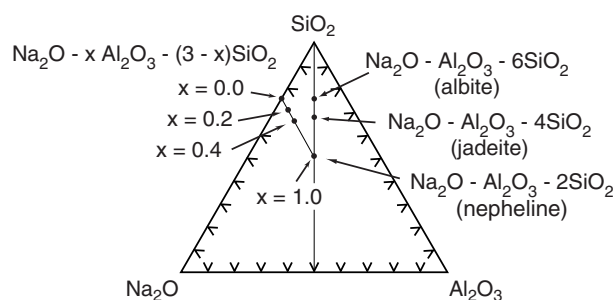


FIGURE 1. In the $\text{Na}_2\text{O}-\text{Al}_2\text{O}_3-\text{SiO}_2$ ternary phase diagram, the $\text{Na}_2\text{O}-\text{Al}_2\text{O}_3-y\text{SiO}_2$ (albite, jadeite, nepheline) join describes fully polymerized glasses formally containing no non-bridging O atoms. Glasses along the $\text{Na}_2\text{O}-x\text{Al}_2\text{O}_3-(3-x)\text{SiO}_2$ join have constant sodium concentration and the number of non-bridging O atoms decreases with increased Al content. Glasses from this second series are referred to as $x = 0.2, 0.4$ and 1.0 , where the $x = 1.0$ glass is also the nepheline glass of the first series.

toelectron spectroscopy (XPS), secondary ion mass spectrometry (SIMS), and Fourier transform infrared reflectance spectroscopy (FTIRRS) probe the composition and structure of the reacted glass surfaces. It has been shown that the leaching and dissolution behavior of these sodium aluminosilicate glasses is influenced by their bulk compositions, since the structures of these glasses change considerably as aluminum replaces silicon in the glass network. In leached layers of various glasses, network formers presumably have different states of connectivity, and the network structure in the altered surface may consist of terminal Si-OH and Al-OH, as well as bridging Al-O-Si and Si-O-Si groups. However, there is a lack of experimental evidence characterizing the actual structural units comprising the network of surface layers formed on aluminosilicate glasses during and after dissolution under ambient conditions. In the study reported here, solid-state nuclear magnetic resonance (NMR) spectroscopy is used in the investigation of altered layers of leached sodium aluminosilicates, since NMR can provide information about the local environment of a nucleus regardless of long-range structural disorder of a material.

Solid-state NMR is recognized as a powerful tool for structural elucidation in crystalline and amorphous materials (Fyfe 1984; Eckert 1992), and a number of previous studies have addressed structural issues for silicates and aluminosilicates and their reactions with water (Eckert et al. 1988; Zavel'sky et al. 1988; Kohn et al. 1989; Yang and Kirkpatrick 1989; Kummerlen et al. 1992; Herzog et al. 1994; Glock et al. 1998; Kohn et al. 1998; Xu et al. 1998; Zotov and Keppler 1998; Oglesby and Stebbins 2000; Riemer et al. 2000; Zeng et al. 2000; McManus et al. 2001). Predominantly, these studies have focused on the addition of water to molten aluminosilicate sys-

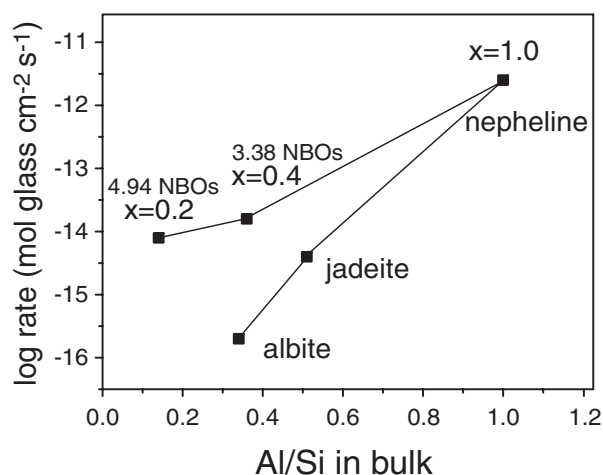


FIGURE 2. Dissolution rates of sodium aluminosilicate glasses leached in aqueous solutions with pH = 2 for 1000 h at 25 °C are shown as a function of bulk Al/Si content. All glasses are expressed as twenty-four O atoms per formula unit. Non-bridging O atom concentrations for $x = 0.2$ and 0.4 glasses per 10 SiO_4 tetrahedra are calculated based on the conventional model (Bruckner et al. 1978; Shelby 1978; Onorato et al. 1985; Goldman 1986; Hsieh et al. 1994; Hsieh and Jain 1995) where each Al atom enters the network and eliminates a NBO up to the ratio of Na/Al = 1.

TABLE 1. Spectrochemical characterization of sodium aluminosilicate glasses and albite crystal*

Composition designation	Na ₂ O mol%	Al ₂ O ₃ mol%	SiO ₂ mol%	Na at%	Al at%	Si at%	O at%	Density (g/cm ³)	NBO/10 SiO ₄ tetrahedra§	Formula unit based on 24 O atoms
$x = 0.2$ glass	24.7	5.3	70.0	15.9	3.4	22.5	58.2	2.452†	4.94	Na _{6.56} Al _{1.40} Si _{9.28} O _{24.00}
$x = 0.4$ glass	25.2	10.4	64.4	15.7	6.5	20.1	57.7	2.476†	3.38	Na _{6.53} Al _{2.70} Si _{8.36} O _{24.00}
nepheline glass ($x = 1.0$ glass)	25.0	25.0	50.0	14.3	14.3	14.3	57.1	2.496†	0.00	Na _{6.01} Al _{6.01} Si _{6.01} O _{24.00}
jadeite glass	16.8	16.9	66.3	10.0	10.1	19.9	60.0	2.431‡	0.00	Na _{4.00} Al _{4.04} Si _{7.96} O _{24.00}
albite glass	12.6	12.7	74.8	7.7	7.8	23.0	61.5	2.382‡	0.00	Na _{3.00} Al _{3.04} Si _{8.96} O _{24.00}
albite crystal	12.2	12.7	74.6	7.5	7.8	22.9	61.5	2.615‡	0.01	Na _{2.93} Al _{3.04} Si _{8.94} O _{24.00}

* Based on lithium metaborate fusion followed by ICP-AES analysis of the resulting solution (Hamilton 1999).

† Day and Rindone 1962.

‡ Taylor and Brown 1979.

§ Based on conventional model that every Al atom enters the network and eliminates an NBO up to the ratio of Na/Al = 1 (Kingery et al. 1976; Bruckner et al. 1978; Onorato et al. 1985; Goldman 1986; Hsieh et al. 1994; Hsieh and Jain 1995; Shelby 1978).

TABLE 2. Dissolution rates of sodium aluminosilicate glasses at pH = 2 and 25 °C

Composition designation	Initial surf. area (cm ² /g)	Initial pH	Final pH	Reaction time (h)	Log dissolution rate (moles Si/cm ² /s)	Log dissolution rate (moles glass/cm ² /s)*
$x = 0.2$ glass	583	2.00	2.11	816	-14.2 ± 0.1	-15.2 ± 0.1
$x = 0.4$ glass	791	2.00	2.03	811	-14.0 ± 0.1	-14.9 ± 0.1
nepheline glass ($x = 1.0$ glass)	891	2.00	2.61	313	-11.9 ± 0.1	-12.7 ± 0.1
jadeite glass	644	2.00	2.11	816	-13.5 ± 0.1	-14.4 ± 0.1
albite glass	705	2.00	2.05	864	-14.7 ± 0.1	-15.7 ± 0.1

* Normalized dissolution rates are expressed as mol glass/cm²/s, where all glasses are expressed as twenty-four O atoms per formula unit. Powder glass samples were used in dissolution experiments (see Table 1 and Hamilton et al. 2001).

tems. Others have studied the swollen layers of electrode glasses over a range of useful compositions (Herzog et al. 1995; Glock et al. 1998). None have addressed the leaching and dissolution of the glasses considered here under ambient conditions.

Using ²⁷Al MAS, ²⁹Si MAS, ¹H → ²⁹Si cross-polarization MAS (CPMAS), ¹H → ²⁷Al CPMAS, and ²³Na MAS NMR, Yang and Kirkpatrick (1989) studied the products of hydrothermal reactions of albite and a near-albite composition glass. Under hydrothermal conditions (250 °C) and pH conditions ranging from 1 to 9, no surface layers were detected on albite crystals, leading to the conclusion that no surface layers of thickness greater than 30 Å are formed under the conditions considered. For glass samples, however, structural changes in a surface layer and the bulk of the glasses are documented, implicating and elucidating the roles of cation exchange and incorporation of molecular water as a function of treatment conditions. For example, the coordination of aluminum in the secondary phases formed under hydrothermal conditions varies from octahedral toward increasing tetrahedral coordination as the pH of the solution increases (Yang and Kirkpatrick 1989). This paper points out the utility of CPMAS NMR for the study of hydrated phases. Similar studies of hydrous albite glasses (Grey and Veeman 1992; Zeng et al. 1999; Zeng et al. 2000), also utilizing more advanced techniques such as Transfer of Populations in Double Resonance (TRAPDOR) NMR (Grey and Veeman 1992) and ²³Na off-resonance nutation NMR spectroscopy (Kohn et al. 1998), have yielded valuable insight into structural issues in these systems.

Herzog and coworkers have studied the hydrated layers of silicate (Herzog et al. 1994) and aluminosilicate (Herzog et al. 1995) electrode glasses with a variety of sophisticated solid-state NMR methods, including Rotational-Echo Double-Resonance (REDOR) NMR (Gullion and Schaefer 1989). Their results demonstrate the usefulness of REDOR as a tool for elucidating structure in these systems, especially with regard to

the coordination of Al by hydroxyl and water species.

It is clear that when used to observe and interrogate selectively the leached layers on glass and mineral samples, polarization transfer NMR experiments are a powerful and effective tool. Other surface sensitive techniques (such as SIMS depth profiling) have shown for the leached glasses studied here that all detectable protons are present near the surface (Hamilton and Pantano 1997; Hamilton et al. 2000; Hamilton et al. 2001). Therefore, ¹H → ²⁹Si and ¹H → ²⁷Al CPMAS NMR, and ¹H/²⁹Si/²⁷Al cross-polarization transfer of populations via double-resonance (CP-TRAPDOR) experiments are used here to provide structural information about silicon and aluminum environments in the altered layers. Using these techniques, transformation of Al from four to sixfold coordination is documented after leaching and alteration of the surface layers of glasses and of albite crystal. ²⁹Si MAS, ²⁷Al MAS, and ²⁷Al → ²⁹Si CPMAS NMR experiments additionally describe the bulk network structures in aluminosilicates, and when compared to results from polarization transfer experiments, these spectra provide further identification of structural units present in the surface layer after dissolution that are not detectable in the bulk. In certain instances, repolymerization of the silicon network via formation of additional Q⁴ silicon sites is observed in samples of leached glasses.

EXPERIMENTAL METHODS

Sample preparation

Two sets of glasses with mole ratios Na₂O:*x*Al₂O₃:(3-*x*)SiO₂ (where *x* = 0.2, 0.4, and 1.0) and Na₂O:Al₂O₃:*y*SiO₂ (where *y* = 2, 4, 6) were prepared. The glass with *x* = 1.0 corresponds to the *y* = 2 glass as shown in Figure 1. The raw materials for glass melting consisted of Min-U-Sil SiO₂, reagent-grade Al(OH)₃, and anhydrous Na₂CO₃ and Na₂SO₄ powders. The raw materials were mixed and melted in platinum crucibles at tem-

peratures ranging from 1550 to 1750 °C in air. After melting for 24 hours, glasses were poured into graphite or stainless steel molds to form bars. The glasses were annealed overnight at temperatures ranging from 520 to 750 °C and then were cooled slowly to room temperature (Hamilton 1999). Table 1 contains the results of spectrochemical analyses of the five glasses discussed in this study. All glass compositions were checked for crystallinity by X-ray diffraction (XRD); no crystalline peaks were observed.

High purity Amelia albite crystals from the Amelia Courthouse, Virginia locality (Wards Scientific) were used in this study. Clear crystals with a high degree of homogeneity were picked by hand. Spectrochemical analyses of powdered specimens (based on a lithium metaborate fusion process followed by ICP-AES analysis of the resulting solution) and electron microprobe analyses of polished crystals indicated only minor deviations from stoichiometric albite, as previously reported by Hamilton et al. (2000).

All samples were dry-crushed to a 74–149 μm grain size in an agate mortar, subsequently cleaned in high-purity acetone, and dried at 60 °C overnight. These powders were placed in 2 L high-density polyethylene (HDPE) containers and immersed in 2300 mL of aqueous solution for 500 or 1000 hours. The containers were placed in an oven maintained at 25 ± 1 °C without agitation. The glass surface area to solution volume ratio (SA/V) was approximately 1.4–2.0 cm^{-1} for each experiment. Unbuffered, aqueous solutions at pH 2 were prepared with trace metal grade HCl and reverse osmosis-filtered (RO) water. The dissolution rates of the samples were calculated from the rate of release of Si to solution, and these results have been reported and commented on previously (Hamilton 1999; Hamilton et al. 2001). After reaction, powders were suction filtered (0.4 μm filter paper), rinsed several times with deionized water, cleaned in an ultrasonic bath in high-purity acetone, and dried at 50 °C overnight. Supernatant solutions were saved to test whether freshly ground glass powder surfaces easily adsorbed dissolved aluminum from the solution. The aluminum concentrations in supernatant solutions were previously measured (Hamilton 1999) using a Leeman Labs PS 3000UV inductively coupled plasma atomic emission spectrometer.

Solid state NMR experiments

^{27}Al MAS and $^1\text{H} \rightarrow ^{27}\text{Al}$ CPMAS NMR spectra shown in Figure 3 were acquired with a Chemagnetics Infinity 500 spectrometer operating at a magnetic field strength of 11.7 T. The ^{27}Al and ^1H resonance frequencies at this field strength are 130.162 MHz and 499.625 MHz, respectively. The reported chemical shift values for ^{27}Al are expressed in ppm and externally referenced to the ^{27}Al resonance from a 1M $\text{Al}(\text{NO}_3)_3$ solution. The $^1\text{H} \rightarrow ^{27}\text{Al}$ CPMAS experiments were performed using samples packed into 5 mm rotors (outer diameter size) and spun at a sample rotational frequency of 4.5 kHz in a double resonance Chemagnetics CPMAS NMR probe. A sample of boehmite (Catapal B) was used to establish the optimum matching condition for the CP experiments. A 0.3 μs contact time and $\pi/2$ pulse width of 5 μs were used, with a recycle delay of one second between acquisitions.

$^1\text{H} \rightarrow ^{27}\text{Al}$ CPMAS NMR data shown in Figures 4 and 5

were acquired using a Chemagnetics CMX-300 spectrometer operating at a magnetic field strength of 7.0 T. The ^{27}Al and ^1H resonance frequencies at this field strength are 77.484 and 297.370 MHz respectively. Sample rotors with a 7.5 mm outer diameter were spun at 3.5 kHz. CP contact pulses of 0.25 μs were used, and the ^1H $\pi/2$ pulse lengths were 5.5 μs . The reported chemical shift values for ^{27}Al are again referenced to a 1M $\text{Al}(\text{NO}_3)_3$ solution.

Since the cross-polarization technique is not useful for the absolute quantification of different aluminum sites, the relative ratios of six and fourfold aluminum in the hydrated layers of leached samples were calculated from the peak areas in $^1\text{H} \rightarrow ^{27}\text{Al}$ CPMAS spectra. Importantly, all data that are compared in Figures 6 and 7 were obtained under precisely controlled and reproducible spectrometer conditions, such that the results are internally quantifiable in the manner used (as a ratio of six-coordinate aluminum species to the total aluminum detected by CPMAS NMR in the surface layer).

$^{27}\text{Al} \rightarrow ^{29}\text{Si}$ CPMAS experiments were performed with a homebuilt NMR spectrometer (9.4 T magnetic field) controlled by a Tecmag pulse programmer. Double resonance experiments

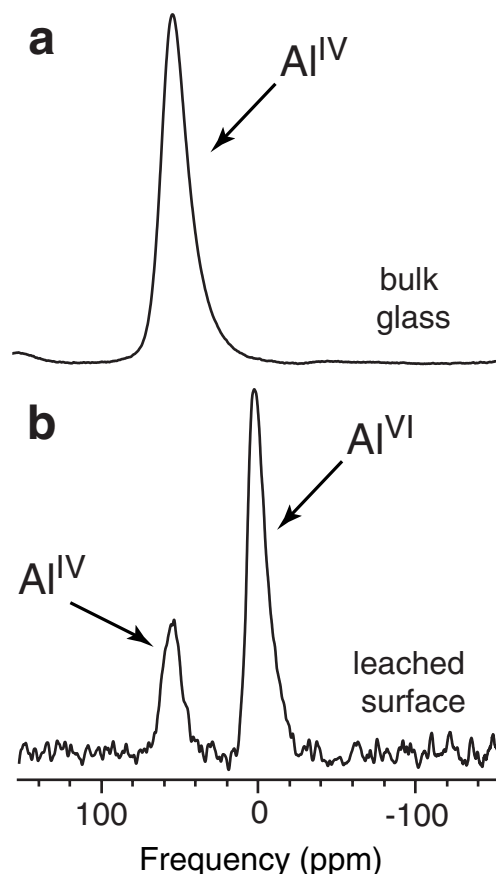


FIGURE 3. (a) The ^{27}Al MAS spectrum of a nepheline glass powder sample leached at pH = 2 for 1000 h shows only the Al^{IV} species present in the bulk of the sample. (b) The $^1\text{H} \rightarrow ^{27}\text{Al}$ CPMAS spectrum of nepheline glass leached at pH = 2 for 1000 h contains resonances from both Al^{IV} and Al^{VI} species present in the altered surface layer.

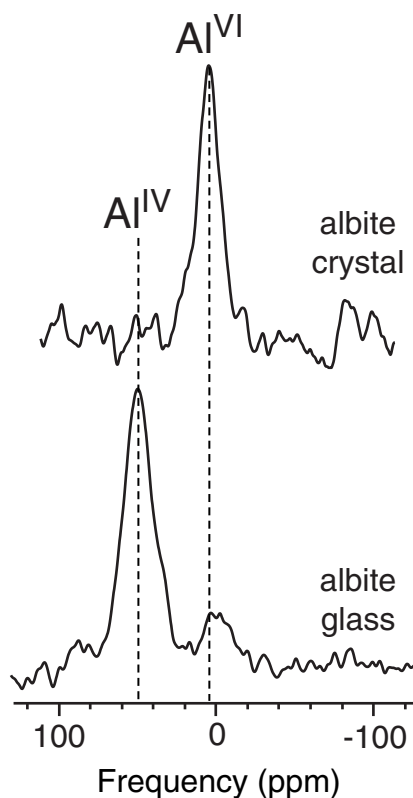


FIGURE 4. The ${}^1\text{H} \rightarrow {}^{27}\text{Al}$ CPMAS spectra of identically leached albite crystal and albite glass, treated at $\text{pH} = 2$ for 1000 h, clearly demonstrate the different coordination environments of aluminum atoms in the leached surface layers of these samples.

were accomplished using the X and Y channels of a Varian/Chemagnetics triple resonance T3 HXY MAS probe. The ${}^{27}\text{Al}$ and ${}^{29}\text{Si}$ resonance frequencies at this magnetic field strength are 104.231 and 79.461 MHz, respectively. Cross-polarization from quadrupolar nuclei such as ${}^{27}\text{Al}$ ($I = 5/2$), is complicated since spin-lock efficiency is affected by the quadrupolar coupling constant, the rotor spinning speed, and the applied spin-lock field. Descriptions of the method and experimental details are found in the literature (DePaul et al. 1997). The transfer of polarization was optimized experimentally for the most efficient spin-lock conditions for the quadrupolar ${}^{27}\text{Al}$ nucleus. The best spin-lock level for the ${}^{27}\text{Al}$ resonance was found to be 2.8 kHz rf field strength. The selective $\pi/2$ pulse length on the aluminum central transition was 83 μs , which corresponds to an rf field strength of 3 kHz. A 1.0 ms contact time was used for all samples. The 7.5 mm diameter MAS rotors were spun at 4 kHz, and the delay between acquisitions was 0.25 seconds.

${}^1\text{H} \rightarrow {}^{29}\text{Si}$ CPMAS NMR spectra were also acquired with the homebuilt NMR spectrometer (9.4 T magnetic field, Tecmag pulse programming system) described above. The ${}^1\text{H}$ resonance frequency at this field strength is 399.991 MHz. Samples were contained in 7.5 mm diameter rotors and spun at 4 kHz. A ${}^{29}\text{Si}$ $\pi/2$ pulse length of 7 μs was used, with an RF field strength of 72 kHz for ${}^1\text{H}$ decoupling during acquisition. The optimal cross-polarization contact time was 3 μs , with a recycle delay of 3 s

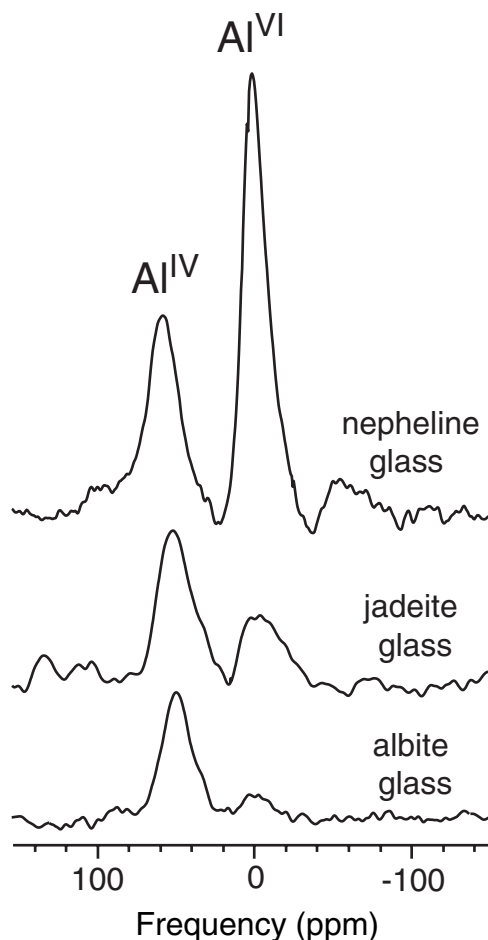


FIGURE 5. The ${}^1\text{H} \rightarrow {}^{27}\text{Al}$ CPMAS spectra of leached albite, jadeite, and nepheline glasses demonstrate a variation in both the amount of overall signal detected and the relative amounts of six- and four-coordinated aluminum detected in the altered layers.

between scans. All reported chemical shift values for ${}^{29}\text{Si}$ are referenced to TMS using solid tetrakis(trimethylsilyl) silane as a secondary reference.

${}^{29}\text{Si}$ MAS NMR spectra and ${}^1\text{H}/{}^{29}\text{Si}/{}^{27}\text{Al}$ CP-TRAPDOR data were acquired with the Chemagnetics CMX-300 spectrometer described above, where the ${}^{29}\text{Si}$ Larmor frequency at this field strength is 59.075 MHz. The pulse sequence used for the CP-TRAPDOR experiment, as well as a further description of the method, have been reported in earlier publications (Grey and Vega 1995; Kao and Grey 1996). ${}^{29}\text{Si}$ magnetization was prepared via ${}^1\text{H} \rightarrow {}^{29}\text{Si}$ cross-polarization after a 5 μs $\pi/2$ pulse was applied to the protons. The optimal contact time for CP was found to be 3 μs . The pulse length for the π refocusing pulse that produced a ${}^{29}\text{Si}$ spin echo of maximum intensity was 12 μs . In the TRAPDOR experiment, the time domain signal leading to the TRAPDOR spectrum is acquired as a difference signal between ${}^1\text{H} \rightarrow {}^{29}\text{Si}$ CP echo signals without (S_0) and with (S_i) on-resonance ${}^{27}\text{Al}$ irradiation. In the S_i portion of the experiment, a long pulse is applied at the resonance frequency of the ${}^{27}\text{Al}$ nuclei during both the dephasing and refocusing peri-

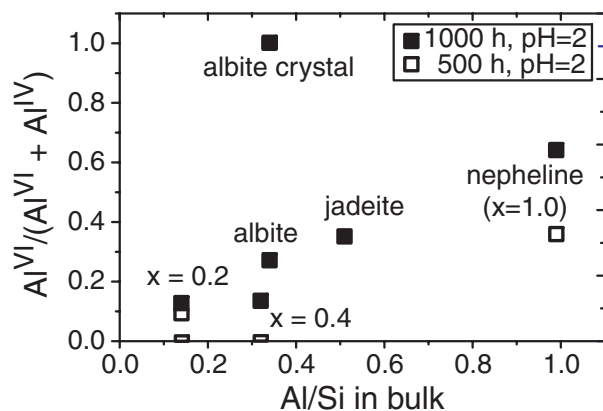


FIGURE 6. The relative amounts of sixfold coordinated Al in the hydrated glass surfaces, determined from $^1\text{H} \rightarrow ^{27}\text{Al}$ CPMAS NMR spectra, are plotted as a function of Al/Si ratio in bulk glass and crystalline samples.

ods of the spin echo. TRAPDOR experiments on nepheline glass were performed with ^{27}Al irradiation for either 4 or 10 rotor cycles, which at 3 kHz spinning speed correspond to 1.33 μs and 3.33 μs of irradiation. The ^{27}Al pulses used in the S_f portion of the experiment had an rf field strength of 41.6 kHz.

RESULTS

^{27}Al MAS and $^1\text{H} \rightarrow ^{27}\text{Al}$ CPMAS NMR

Solid-state NMR is the method of choice for determining the coordination of O atoms around aluminum atoms in amorphous systems, since this technique is sensitive to the local environments of the ^{27}Al nuclei. Initially, single pulse ^{27}Al MAS experiments (with ^1H decoupling) were performed on leached and unleached powder samples. These experiments are not surface selective (since no polarization transfer from ^1H nuclei is occurring) and clearly indicate that aluminum has a tetrahedral coordination (Al^{IV}) in the bulk before and after dissolution for all compositions of glasses and the crystalline albite sample studied. To illustrate this result, Figure 3a shows the ^{27}Al MAS spectrum of a bulk nepheline glass powder after leaching. The resonance line at 57 ppm corresponds to Al^{IV} , and there is no detectable octahedrally coordinated aluminum (Al^{VI}), which would present a resonance at approximately 0 ppm.

All aluminosilicates in our study are systems with no detectable protons in the bulk structure, i.e., no signal has been detected by $^1\text{H} \rightarrow ^{27}\text{Al}$ CPMAS NMR experiments on freshly ground, unleached powder samples. During leaching, hydrated layers of varying degree are formed on the surfaces (Hamilton et al. 2000; Hamilton et al. 2001). Therefore, all detectable protons in the system are present at the surface, and $^1\text{H} \rightarrow X$ ($X = ^{29}\text{Si}, ^{27}\text{Al}$) CPMAS becomes a successful surface-selective technique. $^1\text{H} \rightarrow ^{27}\text{Al}$ CPMAS experiments then provide information about the local environment of the surface aluminum in leached sodium aluminosilicates. As shown in Figure 3b, the $^1\text{H} \rightarrow ^{27}\text{Al}$ CPMAS spectrum of leached nepheline glass shows four and sixfold aluminum coordination in the hydrated layer

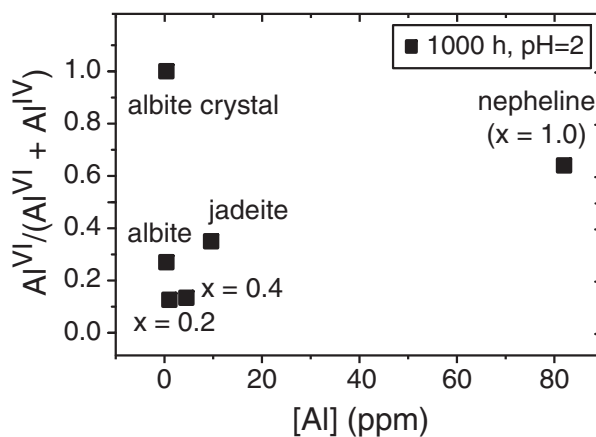


FIGURE 7. The relative amounts of sixfold coordinated Al in the hydrated glass surfaces are plotted as a function of aluminum concentration in the filtered (0.4 μm) supernatant solution present after leaching for 1000 h.

of the glass. Similar results were obtained for each glass surface studied; for $x = 0.2, 0.4$ compositions along the $\text{Na}_2\text{O}-x\text{Al}_2\text{O}_3-(3-x)\text{SiO}_2$ join, as well as for mineral glasses, surface Al was found in both six and fourfold coordination after leaching. However, the leached surface of albite crystal showed the presence of aluminum only in octahedral coordination (Al^{VI}) when analyzed immediately after 1000 h of leaching, and also 11.5 months after removal from solution. In Figure 4, $^1\text{H} \rightarrow ^{27}\text{Al}$ CPMAS spectra of identically treated albite glass and crystal are shown, clearly demonstrating the different Al coordinations in the glass and the crystal surface layers. These data document for the first time that Al^{VI} forms on a dissolving feldspar surface under ambient conditions at $\text{pH} = 2$.

Altered layers on leached sodium aluminosilicates have various thicknesses and different chemical compositions, as measured by SIMS and XPS, depending on the initial (bulk) glass composition and structure (Table 3). For comparison, the Al/Si and Na/Si ratios in the bulk glass samples, measured spectrochemically (Hamilton 1999; Hamilton and Pantano 1997; Hamilton et al. 2000; Hamilton et al. 2001), are also listed in Table 3. Previous XPS measurements of the average surface Al/Si ratio indicate that the outermost 90 \AA of leached layers of all samples except nepheline glass are significantly depleted in Al after dissolution at $\text{pH} = 2$ for 1000 hours. Moreover, for two glasses ($x = 0.4$ and jadeite) the Al/Si ratios measured at the surface by XPS were zero. Nevertheless, $^1\text{H} \rightarrow ^{27}\text{Al}$ CPMAS NMR documents the presence of Al in the hydrated layer for both of these samples, where the leached layer is rigorously defined to be that portion of the sample where measurable concentrations of hydrogen atoms are located.

Figure 5 shows the complete $^1\text{H} \rightarrow ^{27}\text{Al}$ CPMAS results for the leached mineral glasses studied along the $\text{Na}_2\text{O}-\text{Al}_2\text{O}_3-y\text{SiO}_2$ join. For these leached glasses, the outermost 90 \AA of the surface is either close to stoichiometric (nepheline) or depleted in Al (albite, jadeite), as measured by XPS (Table 3). It is evident from Figures 5 and 6 that the fraction of Al^{VI} formed on the glass surface during dissolution increases with increasing Al

concentration in the bulk. An approximately linear correlation is observed between the relative ratio of sixfold to total aluminum measured in the surface layer using $^1\text{H} \rightarrow ^{27}\text{Al}$ CPMAS experiments and the Al/Si ratio in the bulk glass (Fig. 6). The fraction of sixfold aluminum in the leached layer after 1000 h leaching also correlates with the measured dissolution rate of the glass samples along the two joins (Fig. 2). However, no correlation was seen between Al coordination and surface Al/Si or Na/Si ratio as measured by XPS (Table 3). Furthermore, the fraction of sixfold coordinated aluminum on albite crystal is anomalously high when compared to the fractions of Al^{VI} calculated from spectra of the glasses.

The concentrations of aluminum in the supernatant solutions were measured previously for all studied compositions in identical experiments after leaching in a pH = 2 solution for 1000 hours (Hamilton 1999). In Figure 7, the aluminum concentrations in the supernatant solutions are compared to the relative ratios of Al^{VI} in the hydrated layers detected by NMR. No simple correlation is observed in this plot.

The fraction of Al^{VI} in the altered layer increased with increasing duration of dissolution for all glasses (two samples of $x = 0.2$ glass, as well as $x = 0.4$ and nepheline glasses) where the time evolution of relative Al coordination in the surface layer was measured at 500 and 1000 h (Fig. 6). The observed $\text{Al}^{\text{VI}}/(\text{Al}^{\text{VI}} + \text{Al}^{\text{IV}})$ ratio was also measured from several identically treated samples as a function of time after removal from solution to check for aging effects. Specifically, before further analysis by NMR, the albite and jadeite glasses were stored in a desiccator for 20 months, and $x = 0.4$, $x = 1.0$ (nepheline) and albite crystal samples were stored for 11.5 months. No evidence for post-leaching transformation of Al^{IV} to Al^{VI} was observed in any sample in these studies. In addition, a more coarse-grained (75–150 μm) sample of $x = 0.4$ glass treated for 500 h at pH 2 was analyzed immediately after treatment and again after 7 months storage in a desiccator. While $^1\text{H} \rightarrow ^{27}\text{Al}$ CPMAS showed tetrahedral aluminum present in the surface layer in both CPMAS experiments, no Al^{VI} was detected in either experiment, consistent with the lack of formation of Al^{VI} during aging. In contrast, preliminary result on one aged powder glass sample suggests the possibility of transformation of

Al^{VI} to Al^{IV} within the leached layer structure after dissolution (data not shown). However, additional experiments are necessary to reproduce this result and determine its repeatability.

$^1\text{H} \rightarrow ^{29}\text{Si}$ CPMAS NMR

Polarization transfer experiments, such as cross-polarization from protons (Pines et al. 1973), are also recognized as superior surface-selective techniques and have been used extensively to investigate silica surfaces (Sindorf and Maciel 1983; Maciel and Ellis 1994). Figure 8 shows $^1\text{H} \rightarrow ^{29}\text{Si}$ CPMAS spectra of a leached albite crystal sample and all sodium aluminosilicate glasses that were leached for 1000 h at pH = 2 in this study. The spectra of $x = 0.2$, 0.4, and nepheline glasses consist of a single broad resonance line, while the $^1\text{H} \rightarrow ^{29}\text{Si}$ CPMAS spectrum of altered jadeite glass shows three distinct sites at -92.1 ppm, -101.4 ppm, and -111.0 ppm. Similarly distinct, yet slightly broader, peaks are also apparent in the spectrum from leached albite glass.

The $^1\text{H} \rightarrow ^{29}\text{Si}$ CPMAS spectrum of the albite crystal spans a range of shifts from -81 ppm to -111 ppm, with a poor signal-to-noise ratio compared to the spectra obtained from an equal number of experimental scans averaged for the other leached samples. The spectra from jadeite and albite glasses show ^{29}Si resonances covering a range from -85 ppm to -120 ppm with similar shifts of the peak maxima. The $^1\text{H} \rightarrow ^{29}\text{Si}$ CPMAS spectrum of nepheline glass is shifted downfield to -93.1 ppm and covers a chemical shift range from -75 ppm to -119 ppm, while CPMAS spectra of the $x = 0.2$ and $x = 0.4$ glasses show almost identical broad resonance lines over a range of chemical shifts from -75 ppm to -119 ppm.

$^{27}\text{Al} \rightarrow ^{29}\text{Si}$ CPMAS NMR

In $^{27}\text{Al} \rightarrow ^{29}\text{Si}$ CPMAS experiments, polarization is transferred from aluminum to silicon atoms via dipolar couplings. Hence the spectrum provides information about ^{29}Si nuclei that are close in space to aluminum nuclei. Since there is no polarization transfer step from ^1H to ^{27}Al in these experiments, the results represent the ^{29}Si nuclei in the bulk of the samples. The distribution of chemical shifts of resonances in $^{27}\text{Al} \rightarrow ^{29}\text{Si}$ CPMAS NMR spectra for the mineral glasses vary by composition and are apparent in the spectra in Figure 9. The peak maximum of the broad, inhomogeneous ^{29}Si resonance line shifts downfield as the amount of aluminum increases in the bulk glass structure from albite to jadeite (by 4.2 ppm) and to nepheline (with an additional shift of 11.5 ppm). As Figure 9 illustrates, the broad, featureless resonance lines of nepheline, jadeite, and albite glasses cover chemical shift ranges from -73 to -98 ppm, -77 to -107 ppm, and -80 to -112 ppm, respectively. Interestingly, peaks in the spectral region normally assigned to $\text{Q}^4(\text{OAl})$ Si sites are detected in the albite sample, showing that under these CP conditions polarization is being transferred beyond the next-nearest neighbor coordination sphere.

$^1\text{H}/^{29}\text{Si}/^{27}\text{Al}$ CP-TRAPDOR

$^1\text{H} \rightarrow ^{29}\text{Si}$ cross-polarization transfer steps were combined with $^{29}\text{Si}/^{27}\text{Al}$ TRAPDOR NMR experiments to further study the structure of the leached layer on nepheline glass. The initial step of this triple resonance experiment, polarization trans-

TABLE 3. Bulk and surface compositions of aluminosilicate samples and $^1\text{H} \rightarrow ^{27}\text{Al}$ CPMAS NMR results

Composition designation	$\text{Al}^{\text{VI}}/(\text{Al}^{\text{VI}} + \text{Al}^{\text{IV}})\ddagger$	Bulk Al/Si*	Bulk Na/Si*	Surface Al/Si†	Surface Na/Si†
$x = 0.2$ glass	0.126	0.15	0.71	0.02	0.01
$x = 0.4$ glass	0.133	0.32	0.78	0	0
nepheline glass ($x = 1.0$ glass)	0.641	1.00	0.96	0.81	0.65
jadeite glass	0.352	0.51	0.50	0	0
albite glass	0.285	0.34	0.33	0.03	0.01
albite crystal	1	0.34	0.33	0.08	0.07

* Bulk ratios refer to compositions measured spectrochemically (based on lithium metaborate fusion followed by ICP-AES analysis of the resulting solution) for the bulk powders of unreacted glasses (Hamilton 1999).

† Surface ratios refer to compositions of glass plates measured using X-ray photoelectron spectroscopy on the upper 90 Å of surface after dissolution in pH = 2 for 1000 h (Hamilton 2001).

‡ Relative ratio of sixfold aluminum on the altered surface of leached aluminosilicates calculated from the peak areas of $^1\text{H} \rightarrow ^{27}\text{Al}$ CPMAS NMR spectra acquired with the same spectrometer settings and verification of reproducibility of results.

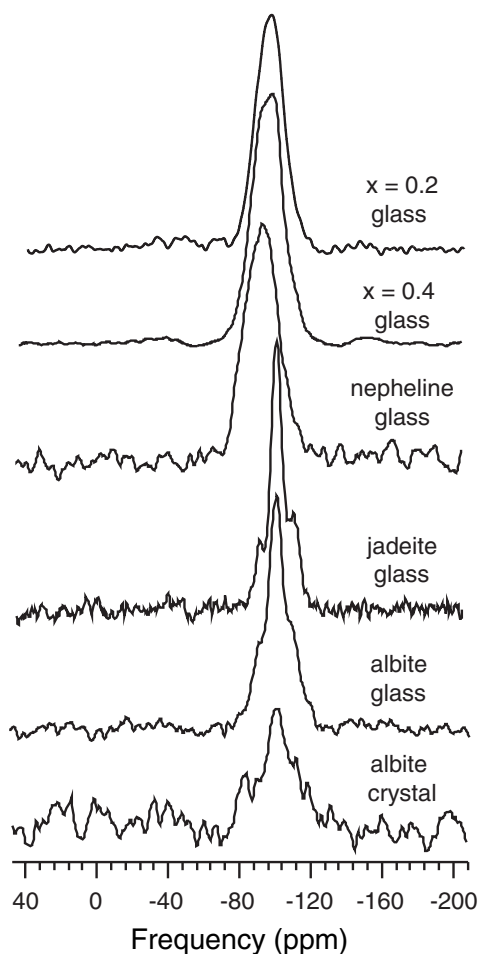


FIGURE 8. The $^1\text{H} \rightarrow ^{29}\text{Si}$ CPMAS NMR spectra of sodium aluminosilicates leached in pH = 2 solution for 1000 hours reveal resonances from ^{29}Si nuclei in the leached layers.

fer from ^1H nuclei to ^{29}Si , provides selective observation of silicon atoms in the hydrated surface layer of the glass. The cross-polarization is followed by $^{29}\text{Si}/^{27}\text{Al}$ double-resonance experiments to select specific ^{29}Si species with close proximity to ^{27}Al within the leached layers.

Spectra from $^1\text{H}/^{29}\text{Si}/^{27}\text{Al}$ CP-TRAPDOR NMR experiments performed on nepheline glass are shown in Figure 10. TRAPDOR signals were acquired for two different evolution times (after 4 and 10 complete rotor cycles). The resonance line observed after 4 rotor periods of ^{27}Al irradiation covers a ^{29}Si chemical shift range from -72.6 to -98.2 ppm. However, the same experiment performed with a longer ^{27}Al pulse (10 rotor cycles) shows a TRAPDOR effect even above -100 ppm, with an overall spread of this broad resonance line from -72 to -115 ppm. For comparison, the ^{29}Si MAS and $^1\text{H} \rightarrow ^{29}\text{Si}$ CPMAS spectra from the same sample are shown.

DISCUSSION

Coordination of Al in leached layers

Given that the sodium aluminosilicates studied here contain only tetrahedral aluminum (Al^{IV}) in the bulk, Al^{VI} on the

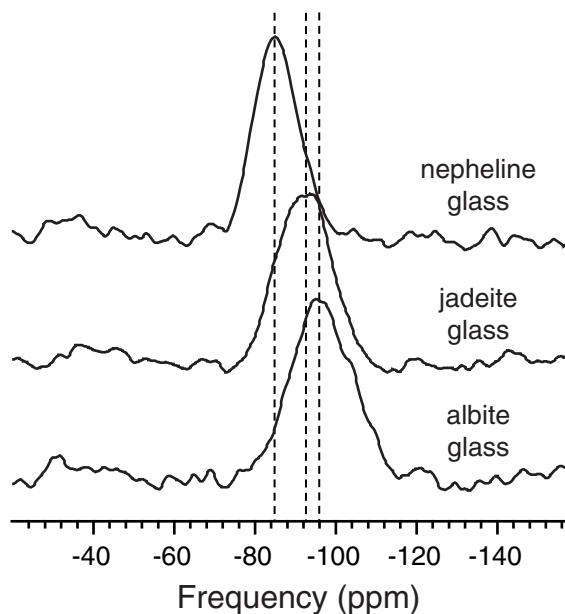


FIGURE 9. The $^{27}\text{Al} \rightarrow ^{29}\text{Si}$ CPMAS spectra of nepheline, jadeite, and albite glasses represent bulk (non-surface) silicon species that are close in space to aluminum nuclei. The dashed lines at the peak maxima are drawn as guides for the eye.

surface after dissolution must derive from either (1) transformation of the glass network (mineral lattice) during leaching; (2) adsorption of sixfold Al from solution; or (3) precipitation of octahedral Al on or within the surface layer. If either of the latter two phenomena explained the observations summarized in Table 3, we would expect that the fraction of Al^{VI} in the hydrated layer would increase consistently with increasing concentration of dissolved Al in solution. As shown in Figure 7, however, no strong correlation is observed. Moreover, supernatant solution analyses have indicated (Hamilton 1999) that dissolved Al concentrations were not close to saturation with respect to Al phases such as gibbsite [$\text{Al}(\text{OH})_3$] or kaolinite [$\text{Al}_2\text{Si}_2\text{O}_5(\text{OH})_4$]. Therefore, precipitation of phases with octahedral aluminum from the solution is highly unlikely. To check whether the glass surface easily adsorbs Al^{VI} from the solution, freshly ground powders of the $x = 0.2$ and 0.4 glasses were placed for 48 h in supernatant solutions of the same glass compositions leached at pH = 2 for 1000 h. $^1\text{H} \rightarrow ^{27}\text{Al}$ CPMAS experiments performed on these samples showed only tetrahedral aluminum with protonated environments for these glass surfaces.

The transformation of Al from four to sixfold is inferred to occur during leaching and alteration of the surface layer. Hence, it is reasonable to search for a correlation between surface chemistry and Al coordination in the leached layer. In fact, as demonstrated in Figure 6, the fraction of Al^{VI} increases monotonically and approximately linearly as the Al content increases in the bulk glasses, but does not scale with the amount of Al in the outermost (90 \AA) surface layer of the glass per se (since there is no correlation with the Al concentration measured in the layer by XPS). This result suggests that bulk composition and structure controls the ultimate coordination of

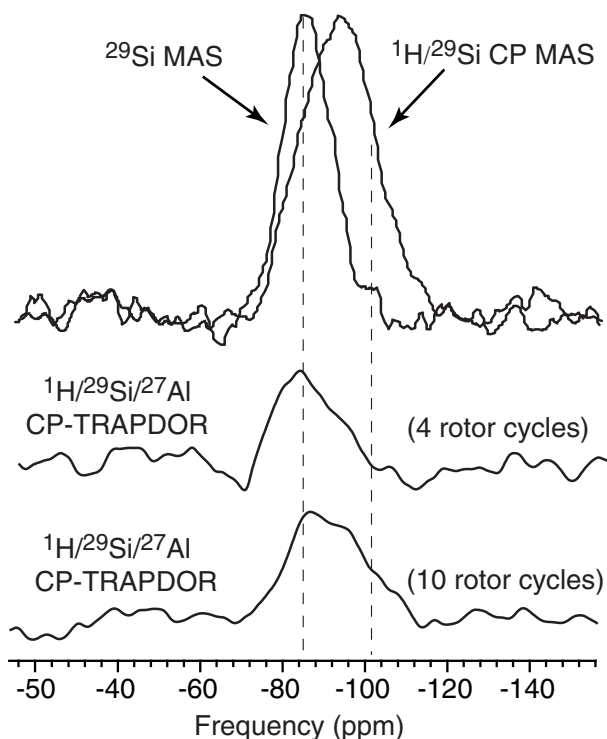


FIGURE 10. ^{29}Si spectra are presented from different NMR experiments performed on the nepheline glass sample leached in pH = 2 solution for 1000 hours at 25 °C. The overlapped lines at the top correspond to ^{29}Si MAS and $^1\text{H} \rightarrow ^{29}\text{Si}$ CPMAS spectra. $^1\text{H} \rightarrow ^{29}\text{Si}$ CP transfers combined with $^{29}\text{Si}/^{27}\text{Al}$ TRAPDOR experiments produce the resonances shown for two different TRAPDOR dephasing times (4 and 10 rotor cycles).

aluminum at the glass/leached layer interface or in the depth of the altered layer. The anomalous data for crystalline albite will be discussed within this context.

Since the cross-polarization technique generally is not useful to quantify the absolute concentrations of distinct sites (Stejskal et al. 1977; Vega 1992), it is the change in the relative concentration of Al^{VI} and Al^{IV} sites in the hydrated layers that is observed and relevant here. Furthermore, changes in the relative fractions of tetrahedral and octahedral Al sites with glass/mineral composition are meaningful only with the assumptions that local structural units and dynamics are the same in all samples investigated.

The ratio $\text{Al}^{\text{VI}}/(\text{Al}^{\text{VI}} + \text{Al}^{\text{IV}})$ is directly affected by the concentration of Al^{VI} , which is itself a function of the extent of hydrolysis of Al-O-Al (Stebbins and Xu 1997; Stebbins et al. 1999) and Al-O-Si linkages. The concentrations of Al-O-Al and Al-O-Si linkages increase as more Al replaces Si in the glass network, explaining in part why the fraction of Al^{VI} increases with Al/Si ratio of the glasses (Fig. 6). The rupture of aluminite linkages (Barrer and Klinowski 1975; Casey et al. 1988b; Casey and Bunker 1990; Hellmann et al. 1990; Hellmann 1995; Stillings and Brantley 1995; Brantley and Stillings 1997) occurs subsequent to cation exchange between Na^+ and H_3O^+ , and so the creation of a protonic environment

at the network aluminite sites is the first step in the hydrolysis reaction. Assuming that the fourfold coordinated aluminum in the hydrated layer is part of the original (non-hydrolyzed) glass network, then the ratio $\text{Al}^{\text{VI}}/(\text{Al}^{\text{VI}} + \text{Al}^{\text{IV}})$ should correlate with the hydrogen penetration depth on the leached glass surfaces. Deeper penetration is characterized by diffusion of more proton-bearing and H_2O species into the glass surface. In this process, sodium depletion occurs due to the ion exchange, and various protonated sites [e.g., $(\text{AlO}_4)^-\text{H}^+$] are formed at Al-O-Si and Al-O-Al sites in the tetrahedral network. Such protonated units give rise to an Al^{IV} signal in $^1\text{H} \rightarrow ^{27}\text{Al}$ CPMAS experiments. Hydrolysis of bonds associated with the protonated sites causes the breakdown of the glass network and both a decrease in the connectivity and an increase in coordination number of the Al atoms in that layer. A decrease in connectivity of the Al atom (decrease in the number of bridging O atoms around the Al atom) presumably precedes the change in coordination number, but at this point we do not know how many bonds must be broken for Al^{IV} to transform to Al^{VI} . To summarize, the relative ratio $\text{Al}^{\text{VI}}/(\text{Al}^{\text{VI}} + \text{Al}^{\text{IV}})$ is controlled by the relative rates of (1) penetration of H-bearing species into relatively intact glass or crystal (and subsequent formation of protonated Al^{IV} sites); (2) hydrolysis of (primarily) protonated Al-O-Si and Al-O-Al linkages, leading to formation of lower connectivity Al^{IV} sites; (3) transformation of lower connectivity Al^{IV} to Al^{VI} sites; and (4) release of Al^{VI} species to solution.

Simplistically, we might predict that the fraction of Al^{VI} on the surface should increase with decreasing hydration of the surface (decreasing hydrated Al^{IV} sites) and with increasing rate of dissolution (removal of Al^{VI} from the surface). Consistent with this model, a linear correlation is observed between the CPMAS-detected fraction of sixfold coordinated aluminum and bulk Al/Si ratio for glasses along the fully polymerized join (albite, jadeite, and nepheline), as shown in Figure 6. Since along this join the number of NBO sites is zero regardless of Al/Si ratio, the number of Al-O-Si linkages per silicate tetrahedron (predominantly) controls their leaching behavior. Due to the high crosslink density of the mineral glass structures, hydrolysis of aluminite groups is necessary to allow deep penetration of solutes and water into the glass surface. The hydrolysis eventually results in coordination change (from four to sixfold) and release of aluminum to the solution (Casey et al. 1988a; Casey et al. 1988b; Hellmann 1995). For example, the proton penetration depth into jadeite is 0.21 μm , as measured by SIMS, while the aluminum depletion depth on the same sample is also about 0.21 μm (Table 4), indicating that proton penetration for this glass composition is accompanied by release of aluminum due to hydrolysis. For nepheline and albite glasses, hydrated layers are thin and they fall under the sensitivity limits (<200–500 Å) of SIMS experiments used in this study (Table 4). Therefore, we are not able to compare proton penetration and aluminum depletion depths on these leached surfaces. Yet, the formation of such thin hydrated layers on nepheline and albite surfaces indicates that proton-bearing species do not penetrate these glass networks easily without hydrolysis and consequent leaching of aluminum; therefore, a relatively small amount of network aluminum (Al^{IV}) is surrounded by protons in these glass surfaces as compared to

glasses of $x = 0.2$ and 0.4 compositions. Thus, an increase in the relative fraction of surface Al^{VI} with increased bulk aluminum content is clearly observed for the mineral glass samples after dissolution. The $x = 0.2$ and 0.4 glasses are not fully polymerized and do contain NBO sites in the bulk structure. NMR experiments have detected the highest relative amount of Al^{IV} for these two samples after leaching (Table 3), and the change in the fraction of sixfold coordinated surface aluminum is less prominent than the change observed as a function of Al/Si ratio for the mineral glasses (see Fig. 6). For this suite of glasses ($x = 0.2, 0.4$), the NBO concentration strongly influences the leaching behavior and the reaction rate with H_2O and H_3O^+ (Fig. 2). The degree of covalent connectivity in the glass network is one of the controlling factors of the extent and the rate of hydration (Casey and Bunker 1990); hence, for $x = 0.2$ and 0.4 glasses more extensive (1.6 and $0.46 \mu\text{m}$, respectively) hydration of the tetrahedral network occurs *without* leaching of network Al from the depth of the hydrated layers (Table 4 and Fig. 11). Therefore, a greater amount of network aluminum (Al^{IV}) exists in proton-containing environments for these glasses.

For two leached samples ($x = 0.4$ and jadeite), the Al/Si ratios measured at the surface by XPS are negligible (Table 3), yet $^1\text{H} \rightarrow ^{27}\text{Al}$ CPMAS spectra showed measurable amounts of Al located in the leached layer. This discrepancy can be explained by the fact that the proton penetration depths (Table 4) into $x = 0.4$ and jadeite glasses are much greater ($0.46 \mu\text{m}$ and $0.21 \mu\text{m}$, respectively, measured by SIMS) than the 90 \AA probed by XPS. For the $x = 0.4$ glass, the Al depletion depth was 800 \AA as shown in Figure 11 (Hamilton 1999), suggesting that a significant amount of aluminum exists at a much greater depth in the hydrated layer than the outermost 90 \AA . Hence, these deeper species should be the aluminum detected by $^1\text{H} \rightarrow ^{27}\text{Al}$ CPMAS NMR on the leached $x = 0.4$ surface. However, as mentioned above, for the jadeite glass the Al depletion depth, as measured by SIMS, is similar to the proton penetration depth (Table 4); therefore, Al^{VI} detected by $^1\text{H} \rightarrow ^{27}\text{Al}$ CPMAS NMR should be mainly located at the interface of the leached (hydrated) layer and the bulk jadeite glass. Such Al^{VI} in this glass and other glasses could be Al that is bonded within the altered glass network, or could be octahedrally coordinated Al species diffusing from the pristine glass-hydrated layer interface into the solution but trapped in the hydrated layers at the time of sampling. In fact, the observed gradient in the Al profile (SIMS) of jadeite glass supports this hypothesis and shows that significantly depleted levels of Al exist throughout the $0.21 \mu\text{m}$ thick leached layer (Fig. 12). On the other hand, the Al profile for the $x = 0.4$ glass shows no evidence for the presence of Al in the outermost 800 \AA of the leached surface (Fig. 13). It is

possible that the $x = 0.4$ glass, which is not fully polymerized, forms a more open and highly porous altered layer, which provides an easy diffusion pathway for octahedral aluminum species from the glass into solution. An easy diffusion pathway might obviate against trapping octahedral Al within the altered layer.

$^1\text{H} \rightarrow ^{27}\text{Al}$ CPMAS experiments also document different CPMAS-detected fractions of four- and six-coordinated Al on similarly treated glassy and crystalline albite samples, as shown in Figure 4. Only sixfold coordinated Al is detected on the leached albite crystal, whereas on the glass surface a high fraction of tetrahedral aluminum was found. This result can be explained by the fact that much more extensive leaching of sodium has been observed for the glass surface layer compared to the crystal surface layer, even though the thickness of these leached layers were not measurable by SIMS and cannot be compared (Table 4). Moreover, during leaching, the specific surface area increased more profoundly for albite glass relative to the crystal (Hamilton et al. 2000). Consequently, deeper penetration of proton-bearing species is expected on the glass surface, and accordingly, CPMAS NMR detects a higher concentration of network (tetrahedral) aluminum in protonated environments for the albite glass. On the contrary, on albite crystal the hydrogen penetration and consequent surrounding of network (fourfold) Al by protons is less extensive. Therefore, for crystalline albite, the Al^{IV} apparently falls under the detectability limit of CPMAS NMR for the experimental conditions used, and only Al^{VI} is detected. Finally, the albite crystal has a higher density than albite glass (Table 1), and its leached layer has lower po-

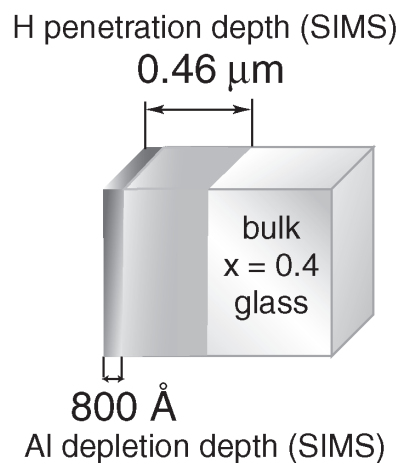


FIGURE 11. A schematic rendering of the layers formed on the surface of the $x = 0.4$ glass during leaching (in $\text{pH} = 2$ solution for 1000 h at $25 \text{ }^\circ\text{C}$) is presented based on data from SIMS analyses.

TABLE 4. SIMS analysis of leached aluminosilicate glass plates

Composition designation	Solution pH	Reaction time (h)	SIMS hydrogen penetration depth	SIMS-measured Al depletion depth	SIMS-measured Na depletion depth
$x = 0.2$ glass	2	619	$1.6 \mu\text{m}$	$\leq 200\text{--}500 \text{ \AA}$	$1.64 \mu\text{m}$
$x = 0.4$ glass	2	1006	$0.46 \mu\text{m}$	800 \AA	$0.45 \mu\text{m}$
nepheline glass ($x = 1.0$ glass)	2	1004	$\leq 200\text{--}500 \text{ \AA}$	$\leq 200\text{--}500 \text{ \AA}$	$\leq 200\text{--}500 \text{ \AA}$
jadeite glass	2	1102	$0.21 \mu\text{m}$	$0.21 \mu\text{m}$	$0.21 \mu\text{m}$
albite glass	2	1000	$\leq 200\text{--}500 \text{ \AA}$	$\leq 200\text{--}500 \text{ \AA}$	$\leq 200\text{--}500 \text{ \AA}$

rosity or openness (Hamilton et al. 2000). This might also inhibit diffusion of the octahedral Al species into solution for crystalline albite.

Structural description of leached layers by ^{29}Si NMR

To investigate the silicon environments in the hydrated layers of the leached sodium aluminosilicate glasses and crystal, polarization transfer techniques were also used, since simple ^{29}Si MAS NMR spectra of silicate glass and mineral powder samples are usually dominated by resonances due to ^{29}Si nuclei in the bulk glass. Since essentially all detectable protons are present within the hydrated surfaces studied here, $^1\text{H} \rightarrow ^{29}\text{Si}$ CPMAS experiments allow selective detection of local Si environments in the leached surface layers.

The $^1\text{H} \rightarrow ^{29}\text{Si}$ CPMAS spectra of the $x = 0.2$ and 0.4 leached glasses show broad, featureless resonance lines (Fig. 8) with similar chemical shift ranges. Such spectra are again not quantifiable and do not yield direct information about relative abundances of the different types of silicon sites. As previously reported by Hamilton et al. (1997), the $x = 0.2$ and 0.4 glass compositions exhibit extensive Si-rich surface layer formation when leached in acid, and show hydrogen penetration depths of 1.6 and 0.46 μm , respectively, after dissolution at $\text{pH} = 2$ for 1000 h (Table 4). Furthermore, for the $x = 0.4$ glass surface, SIMS has demonstrated the presence of Al only in the deeper areas (>800 \AA) of thick hydrated layers; and for the $x = 0.2$ glass only the outermost 200 – 500 \AA is depleted in aluminum (Table 4). Therefore, the peak breadth in the $^1\text{H} \rightarrow ^{29}\text{Si}$ CPMAS spectra of these glasses is due to the existence of a range of different Q^n [i.e., $\text{Si}(\text{OSi})_n(\text{OH})_{4-n}$ where $n = 0, 1, 2, 3$] silicon sites and various overlapping $\text{Q}^n(m\text{Al})$ sites (where Q^n represents a SiO_4 group with n bridging O bonds, and m represents the number of Al atoms per silica tetrahedron) in the altered surface layers.

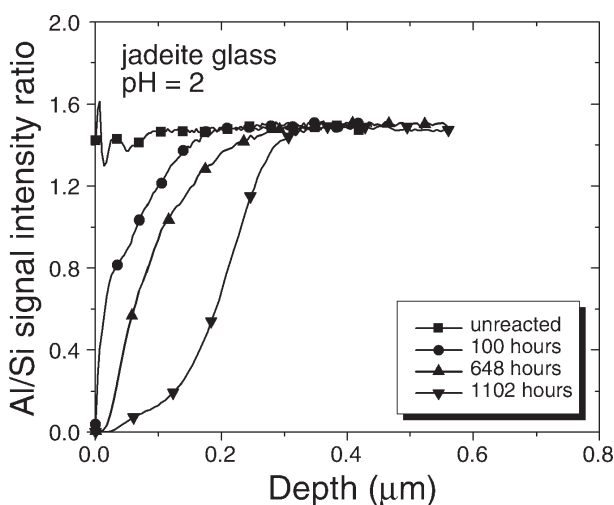


FIGURE 12. SIMS Al depth profiles of jadeite glass reacted at $\text{pH} = 2$ for various lengths of time at 25 $^{\circ}\text{C}$ (Hamilton et al. 2001) show the gradient in Al concentration throughout the leached layer at 1102 h leaching time.

As previously shown by SIMS hydrogen depth profiles of leached albite, jadeite, and nepheline glasses (Table 4), the increase in bulk aluminum concentration from albite to jadeite correlates with a significant increase in the thickness of the hydrated layer. However, with a further increase of Al content (to $\text{Al}/\text{Si} = 1.0$), nepheline glass dissolves rapidly and almost stoichiometrically without formation of a leached layer detectable by SIMS. In addition, FTIRRS analyses have documented that the thick (~ 0.21 μm) hydrated layer on jadeite glass is consistent with a porous, gel type structure (Hamilton et al. 2001). However, no structural transformation was detected on albite and nepheline glass surfaces by FTIRRS since the analysis depth of this technique was greater than 1 μm at 1250 – 900 cm^{-1} ; therefore, bulk structure below the modified surface is dominantly probed by FTIRRS. On the contrary, $^1\text{H} \rightarrow ^{29}\text{Si}$ CPMAS experiments detect silicon signal from hydrated surfaces of all mineral glasses and the crystalline albite studied here (Fig. 8). Comparison of these $^1\text{H} \rightarrow ^{29}\text{Si}$ CPMAS NMR spectra show that albite and jadeite resonance lines are almost identical, indicating that the altered layers formed on these glasses are structurally similar. Therefore, the surface layer on albite glass is likely to be consistent with a porous, gel type structure. Figure 8 also shows the $^1\text{H} \rightarrow ^{29}\text{Si}$ CPMAS spectrum from the leached (polycrystalline) powder of albite. While the poor signal-to-noise ratio is a clear indication of a thinner altered layer formed on the albite crystal compared to the glass, this spectrum still suggests the presence of a hydrated amorphous silicate layer on the leached albite crystal surface, similar to that detected on the albite glass.

However, a different altered layer structure is observed for nepheline glass, as detected by the $^1\text{H} \rightarrow ^{29}\text{Si}$ CPMAS experiment, since the resonance line of nepheline is shifted downfield by 8.6 ppm with respect to resonances in the albite and jadeite spectra. This result is consistent with XPS observations that all glasses except nepheline show significant aluminum depletion

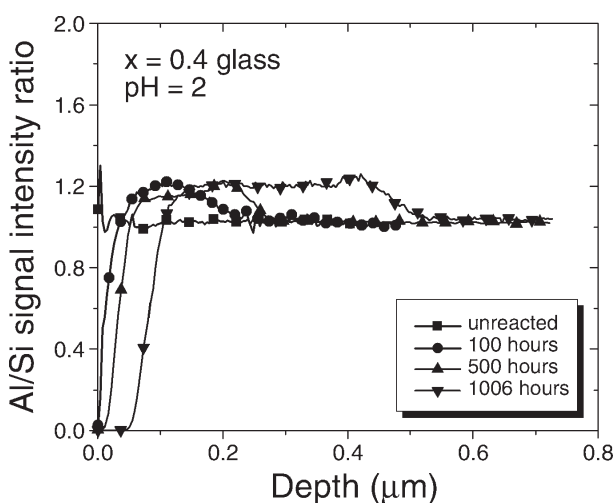
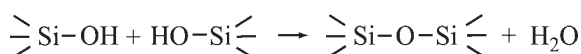


FIGURE 13. SIMS Al depth profiles of $x = 0.4$ glass reacted at $\text{pH} = 2$ for various lengths of time at 25 $^{\circ}\text{C}$ are shown (Hamilton 1999).

from the outermost 90 Å after dissolution. Consequently, the hydrated surface of nepheline has a high aluminum concentration, and therefore the ^{29}Si spectrum obtained selectively from the surface layer of nepheline is deshielded due to an increased number of aluminum next-nearest neighbors to silicon in the leached layer.

The $^{27}\text{Al} \rightarrow ^{29}\text{Si}$ cross-polarization MAS experiments utilize and demonstrate the spatial proximity of ^{27}Al nuclei to silicon atoms in bulk aluminosilicate glasses. Differences between silicon resonances in the bulk structure (as reported by $^{27}\text{Al} \rightarrow ^{29}\text{Si}$ CPMAS and ^{29}Si MAS) and silicon environments in the hydrated surface ($^1\text{H} \rightarrow ^{29}\text{Si}$ CPMAS) will provide further delineation of those structural units formed on the surfaces during dissolution. For the fully polymerized mineral glasses in the series $\text{Na}_2\text{O}-\text{Al}_2\text{O}_3-y\text{SiO}_2$, no Q^n structural units except Q^4 should be a detectable part of the bulk glass network in ^{29}Si NMR experiments. Thus, ^{29}Si spectra of these bulk glasses should only carry information about the range of different $Q^4(m\text{Al})$ (where $m = 0, 1, 2, 3, 4$) structural groups. In the $^{27}\text{Al} \rightarrow ^{29}\text{Si}$ CPMAS spectra shown in Figure 9, the center frequency of the silicon spectra shifts downfield from albite to nepheline. The shift is expected, due to the increased number of Al-O-Si linkages per SiO_4 tetrahedron in the bulk structures. Nevertheless, distinct silicon environments cannot be resolved from these spectra, and the determination of silicon sites with varying numbers of aluminum neighbors from a featureless resonance line is model-dependent. For example, when perfect Al avoidance is assumed, the presence of only $Q^4(4\text{Al})$ species is predicted for nepheline glass. However, Lee and Stebbins (1999) have calculated the distribution function of all five $Q^4(m\text{Al})$ units with respect to degree of Al avoidance for fully polymerized aluminosilicate glasses. Their fitting results for ^{29}Si MAS NMR spectra predict the contributions from each $Q^4(m\text{Al})$ structural unit for various compositions along the $\text{Na}_2\text{O}-\text{Al}_2\text{O}_3-y\text{SiO}_2$ join. However, there was no $Q^4(0\text{Al})$ unit predicted for the nepheline glass structure from the ^{29}Si MAS NMR spectrum, indicating that every detected silicon atom in nepheline has at least one aluminum next nearest neighbor. The ^{29}Si MAS NMR experiment (Fig. 10) shows a broad resonance line associated with all silicon structural units $Q^4(m\text{Al})$ ($m = 1, 2, 3, 4$) of the leached bulk nepheline glass, covering the ^{29}Si chemical shift range from -72.6 to -98.2 ppm. On the contrary, the $^1\text{H} \rightarrow ^{29}\text{Si}$ CPMAS spectrum (Fig. 8), detecting only the silicon atoms in the hydrated layer of nepheline glass, shows ^{29}Si resonances around -108 ppm, corresponding to $Q^4(0\text{Al})$ species. This $Q^4(0\text{Al})$ structural unit did not exist in the bulk glass structure, as clearly shown in Figure 10 by overlapping the $^1\text{H} \rightarrow ^{29}\text{Si}$ and ^{29}Si MAS spectra. This result suggests the formation of $Q^4(0\text{Al})$ silicon sites on nepheline glass during leaching and alteration of the surface in an acidic environment. Formation of $Q^4(0\text{Al})$ species requires condensation of surface silanol groups after leaching of Al. In previous studies (Casey and Bunker 1990; Hellmann et al. 1990; Stillings and Brantley 1995) it was suggested that aging of feldspar powders included formation of Si-O-Si bonds from vicinal silanols as well as a decrease in surface area related to healing of microcracks:



NMR detection of $Q^4(0\text{Al})$ structural units in the surface layer of leached nepheline is evidence strongly supporting the occurrence of such a reaction on the nepheline glass.

The fact that the surface of nepheline is altered through repolymerization raises additional questions about local- and intermediate-range ordering of silicon and aluminum atoms in the altered layer, such as whether the repolymerized areas are phase separated from aluminum-containing areas. To investigate the proximity of the ^{27}Al and the ^{29}Si spins in the altered nepheline surface layers, $^1\text{H} \rightarrow ^{29}\text{Si}$ CP is combined with $^{29}\text{Si}/^{27}\text{Al}$ TRAPDOR experiments. In Figure 10, the bottom two spectra are $^1\text{H}/^{29}\text{Si}/^{27}\text{Al}$ CP-TRAPDOR spectra obtained with 4 and 10 rotor periods of ^{27}Al irradiation. The TRAPDOR effect depends on the dipolar coupling between ^{29}Si and ^{27}Al spins, and stronger local dipolar coupling will cause greater dephasing of ^{29}Si spins during the ^{27}Al pulse. Additionally, for a given dipolar coupling strength, allowing action of the coupling for a longer period of time causes greater loss of signal intensity. A greater loss of the intensity at the ^{29}Si echo is observed through enhanced signal in the TRAPDOR difference spectra shown.

As illustrated in Figure 10, the TRAPDOR difference signal for shorter dephasing times (4 rotor cycles) covers the same ^{29}Si chemical shift range as ^{29}Si MAS NMR spectrum (from -72.6 to -98.2 ppm), indicating short-range dipolar couplings between aluminum and silicon atoms in environments similar to those in the bulk glass. However, when the ^{27}Al irradiation is increased to 10 rotor cycles (3.33 μs), contributions from long-range dipolar interactions are also detectable, and the TRAPDOR effect is observed for ^{29}Si resonances below -100 ppm, indicating that while these $Q^4(0\text{Al})$ Si species do not have Al nuclei as next-nearest neighbors in the structure (as also determined conclusively through their chemical shift values), at least an observable number of $Q^4(0\text{Al})$ Si species are present in phases containing Al in nearby environments. These NMR observations suggest that even though the alteration of the nepheline surface layer does not leave a thick, connected Si-rich layer, silanol groups condense locally into a linked structure. NMR observations documenting Al^{IV} , Al^{VI} , and $Q^4(0\text{Al})$ silicon sites on nepheline thus suggest that Al^{IV} sites first transform to Al^{VI} sites at the surface and then are released to solution. After release of Al^{VI} , silanols condense to form $Q^4(0\text{Al})$ silicon sites. For the nepheline composition, it is also known that the dissolution is near stoichiometric at $\text{pH} = 2$, suggesting that only slight Al leaching gives rise to the different sites documented by NMR. The congruent dissolution of this mineral is similar to the near-stoichiometry of dissolution of anorthite, another aluminosilicate with an Al/Si ratio = 1. Dissolution of anorthite has been characterized by a conceptual model proposed by various authors (Casey et al. 1991; Oelkers and Schott 1995), wherein the removal of aluminum from the surface of anorthite (or, by analogy, nepheline) leaves unconnected silicon structural units that are easily released into solution. However, formation of new siloxane bonds at the leached surface due to condensation of surface silanol groups, as shown by NMR, suggests that in order to fully describe all processes taking place during or after dissolution and alteration of leached layer, more complex models of dissolution are needed, even for compositions where dissolution occurs stoichiometrically.

$^1\text{H} \rightarrow ^{29}\text{Si}$ CPMAS NMR (Fig. 8) has detected well-pronounced ^{29}Si resonances around -110 ppm (corresponding to $\text{Q}^4(\text{OAl})$ silicate tetrahedra) in the leached layers of all studied glass compositions, which is consistent with an extensively connected thick Si-rich layer structure. Because different fractions of $\text{Q}^4(\text{OAl})$ species already exist in the glass network of all sodium aluminosilicates with $\text{Al/Si} < 1$, it is only in the nepheline sample that the repolymerization is unequivocally characterized by these NMR methods. Repolymerization in other cases cannot be ruled out.

Interestingly, aging of glass powders after leaching showed no transformation of Al^{IV} to Al^{VI} but the possibility of Al^{VI} transformation to Al^{IV} was observed in one experiment. The preliminary observation of Al^{VI} transformation to Al^{IV} could be consistent with loss of water due to condensation of aluminol-silanol pairs into Al-O-Si linkages during aging under vacuum. Such a conclusion needs to be investigated further but would be consistent with condensation of both Al and Si atoms occurring in these altered surface layers. On the other hand, transformation of Al^{IV} to Al^{VI} might have been expected if clay-like or gibbsite-like phases crystallized on the glass surfaces during aging, and such crystallization must not be occurring during aging. Reactivity of these altered layers may be important in natural systems where naturally hydrated surfaces may serve as templates for nucleation of new phases (e.g., Nugent et al. 1998).

CONCLUSIONS

The understanding of the mechanisms of feldspar dissolution is enhanced by study of the reactions of aluminosilicate glasses and minerals under relevant ambient conditions. Solid-state NMR studies within two series of sodium aluminosilicate glass powders [$\text{Na}_2\text{O}-x\text{Al}_2\text{O}_3-(3-x)\text{SiO}_2$ and $(\text{Na}_2\text{O}-\text{Al}_2\text{O}_3-y\text{SiO}_2)$ joins], as well as their comparison to similar studies on albite crystal, reveal new information about the structure of the surface layers of these materials. While ^{27}Al and ^{29}Si MAS NMR studies reveal information about the local structures of silicate and aluminate species, cross-polarization from hydrogen atoms within the surface layers provides structural clues to the predominant mechanisms responsible for dissolution, and the variation seen with different bulk structures. Aluminum in octahedral coordination by O atoms (Al^{VI}) is confirmed for the first time on the near-surface region of albite crystal after treatment at $\text{pH} = 2$ for 1000 h at 25°C .

In summary, $^1\text{H} \rightarrow ^{27}\text{Al}$ CPMAS spectra obtained in a manner so as to make quantitative comparisons, demonstrate the presence and evolution of Al^{VI} species within the hydrated layers formed during leaching at $\text{pH} 2$ on all glasses and minerals studied here. It is shown for all the glass samples that the fractions of Al^{VI} in the layers increase as the amount of aluminum in the bulk of the glass increases. This observation implicates a mechanism where the concentration of aluminum controls the end-products of the dissolution mechanism. $^1\text{H} \rightarrow ^{29}\text{Si}$ CPMAS spectra are also informative as to the extent of surface reactions of silicate species as other atoms are removed from the surface layers, and a silica gel-type layer (similar to that deduced previously for jadeite glass) is consistent with new data from albite glass and crystalline samples. In the nepheline glass,

evidence for repolymerization of the silicate network has been presented by comparison of a $^1\text{H} \rightarrow ^{29}\text{Si}$ CPMAS spectrum with ^{29}Si MAS data from the bulk glass. A TRAPDOR NMR experiment coupled with $^1\text{H} \rightarrow ^{29}\text{Si}$ CPMAS provides a measure of the spatial proximity of the repolymerized $\text{Q}^4(\text{OAl})$ silicate species with aluminum atoms in the surface layer, addressing in part whether these units are phase-separated from aluminate species in the surface layer. This battery of solid-state NMR experiments has been effectively coupled with measurements of the localization of hydrogen atoms (as the working definition of the surface layers in these systems), the depletion depths of aluminum species, and data such as dissolution rates. Interpretation of this variety of data present a detailed analysis of structure and chemistry in the surface layers of a range of sodium aluminosilicate glasses and crystalline albite treated for 1000 h in an aqueous solution with a pH of 2 at ambient temperatures.

Furthermore, these NMR spectra elucidate some of the many processes occurring during leaching of aluminosilicate glasses and crystals as the altering surface layer reaches steady state. Apparently, the transient early dissolution of an aluminosilicate causes topographic changes on the mineral surface (e.g., Mellott et al. 2002) as well as coordination changes for both Al and Si as shown here.

ACKNOWLEDGMENTS

This work was supported in part with a grant to KTM from the National Science Foundation Industry-University Center for Glass Research, which is funded through research grant NSF-E9908423. This research was supported by the Department of Energy (DE-FG02-95ER14547.A000) in funding to SLB and CGP. KTM wishes to thank the Camille Dreyfus Teacher-Scholar program for additional financial support. NMR instrumentation used in this research was obtained through grants from the National Science Foundation (CHE-9601572 and DMR-9413674).

The authors also thank D. Aurentz, N. Mellott, H. Gong, and A. Barnes for helpful discussions and assistance with sample preparation.

REFERENCES CITED

- Barrer, R.M. and Klinowski, J. (1975) Hydrogen mordenite and hydronium mordenite. *Journal of Chemical Society Faraday Transactions*, 71, 690–698.
- Blum, A.E. and Lasaga, A.C. (1991) The role of surface speciation in the dissolution of albite. *Geochimica et Cosmochimica Acta*, 55, 2193–2201.
- Blum, A.E. and Stillings, L.L. (1995) Feldspar dissolution kinetics. In S.L. Brantley, Ed., *Chemical Weathering Rates of Silicate Minerals*, 31, p. 291–351. Mineralogical Society of America.
- Brady, P.V. and Walther, J.V. (1989) Controls on silicate dissolution rates in neutral and basic pH solutions at 25-degrees-C. *Geochimica et Cosmochimica Acta*, 53, 2823–2830.
- Brantley, S.L. and Stillings, L. (1996) Feldspar dissolution at 25°C and low pH. *American Journal of Science*, 296, 101–127.
- (1997) Reply: Feldspar dissolution at 25°C and low pH. *American Journal of Science*, 297, 1021–1032.
- Bruckner, R., Chun, H.-U., and Goretzki, H. (1978) Photoelectron spectroscopy (ESCA) on alkali silicate- and soda aluminosilicate glasses. *Glastechnische Berichte*, 51, 1–7.
- Casey, W.H. and Bunker, B. (1990) Leaching of mineral and glass surfaces during dissolution. *Reviews in Mineralogy*, 23, 397–426.
- Casey, W.H., Westrich, H.R., and Arnold, G.W. (1988a) Mechanisms of feldspar dissolution in acid-solutions. *Chemical Geology*, 70, 77–77.
- (1988b) Surface chemistry of labradorite feldspar reacted with aqueous solutions at $\text{pH}=2, 3$, and 12. *Geochimica et Cosmochimica Acta*, 52, 2795–2807.
- Casey, W.H., Westrich, H.R., Arnold, G.W., and Banfield, J.F. (1989) The surface-chemistry of dissolving labradorite feldspar. *Geochimica et Cosmochimica Acta*, 53, 821–832.
- Casey, W.H., Westrich, H.R., and Holdren, G.R. (1991) Dissolution rates of plagioclase at $\text{pH} = 2$ and 3. *American Mineralogist*, 76, 211–217.
- Day, D.E. and Rindone, G.E. (1962) Properties of soda aluminosilicate glasses: I, refractive index, density, molar refractivity, and infrared absorption spectra. *Journal of the American Ceramic Society*, 45, 489–496.

- DePaul, S.M., Ernst, M., Shore, J.S., Stebbins, J.F., and Pines, A. (1997) Cross-polarization from quadrupolar nuclei to silicon using low-radio-frequency amplitudes during magic-angle spinning. *Journal of Physical Chemistry B*, 101, 3240–3249.
- Eckert, H. (1992) Structural characterization of noncrystalline solids and glasses using solid state NMR. *Progress in NMR Spectroscopy*, 24, 159–293.
- Eckert, H., Yesinowski, J.P., Silver, L.A., and Stolper, E.M. (1988) Water in silicate-glasses—quantitation and structural studies by H-1 solid echo and MAS-NMR methods. *Journal of Physical Chemistry*, 92, 2055–2064.
- Fyfe, C.A. (1984) *Solid State NMR for Chemists*. CFC Press, Guelph.
- Glock, K., Hirsch, O., Rehak, P., Thomas, B., and Jager, C. (1998) Novel opportunities for studying the short and medium range order of glasses by MAS NMR, Si-29 double quantum NMR and IR spectroscopies. *Journal of Non-Crystalline Solids*, 234, 113–118.
- Goldman, D.S. (1986) Evaluation of the ratios of bridging to nonbridging oxygens in simple silicate-glasses by electron-spectroscopy for chemical-analysis. *Physics and Chemistry of Glasses*, 27, 128–133.
- Grey, C.P. and Veeman, W.S. (1992) The detection of weak heteronuclear coupling between spin 1 and spin 1/2 nuclei in MAS NMR; $^{14}\text{N}/^{13}\text{C}/^1\text{H}$ triple resonance experiments. *Chemical Physics Letters*, 192, 379–385.
- Grey, C.P. and Vega, A.J. (1995) Determination of the quadrupole coupling-constant of the invisible aluminum spins in zeolite HY with H-1/Al-27 TRAPDOR NMR. *Journal of the American Chemical Society*, 117, 8232–8242.
- Gullion, T. and Schaefer, J. (1989) Rotational-echo double-resonance. *Journal of Magnetic Resonance*, 81, 196–200.
- Hamilton, J.P. (1999) Effects of structure, composition, and pH on the corrosion behavior of sodium-aluminosilicate glasses and crystals. Ph.D. dissertation, Penn State University.
- Hamilton, J.P. and Pantano, C.G. (1997) Effects of glass structure on the corrosion behavior of sodium-aluminosilicate glasses. *Journal of Non-Crystalline Solids*, 222, 167–174.
- Hamilton, J.P., Pantano, C.G., and Brantley, S.L. (2000) Dissolution of albite glass and crystal. *Geochimica et Cosmochimica Acta*, 64, 2603–2615.
- Hamilton, J.P., Brantley, S.L., Pantano, C.G., Criscenti, L., and Kubiki, J. (2001) Dissolution of nepheline, jadeite and albite glasses: toward better models for aluminosilicate dissolution. *Geochimica et Cosmochimica Acta*, 65, 3683–3702.
- Hellmann, R. (1995) The albite-water system. II. The time-evolution of the stoichiometry of dissolution as a function of pH at 100-degrees-C, 200-degrees-C, and 300-degrees-C. *Geochimica et Cosmochimica Acta*, 59, 1669–1697.
- Hellmann, R., Eggleston, C.M., Hochella, M.F., and Crerar, D.A. (1990) The formation of leached layers on albite surfaces during dissolution under hydrothermal conditions. *Geochimica et Cosmochimica Acta*, 54, 1267–1281.
- Hellmann, R., Dran, J.C., and DellaMea, G. (1997) The albite-water system. III. Characterization of leached and hydrogen-enriched layers formed at 300 degrees C using MeV ion beam techniques. *Geochimica et Cosmochimica Acta*, 61, 1575–1594.
- Herzog, K., Scholz, K., and Thomas, B. (1994) Structure of Hydrated Layers on Silicate Electrode Glasses. *Solid State Nuclear Magnetic Resonance*, 3, 1–15.
- Herzog, K., Thomas, B., Sprenger, D., and Jager, C. (1995) REDOR NMR: approaching structural elucidation of hydrated layers in silicate electrode glasses. *Journal of Non-Crystalline Solids*, 190, 296–300.
- Hsieh, C.H. and Jain, H. (1995) Influence of network-forming cations on ionic-conduction in sodium-silicate glasses. *Journal of Non-Crystalline Solids*, 183, 1–11.
- Hsieh, C.H., Jain, H., Miller, A.C., and Kamitsos, E.I. (1994) X-ray photoelectron spectroscopy of Al- and B- substituted sodium trisilicate glasses. *Journal of Non-Crystalline Solids*, 68, 247–257.
- Kao, H.M. and Grey, G.P. (1996) Probing the Bronsted and Lewis acidity of zeolite HY: A H-1/Al-27 and N-15/Al-27 TRAPDOR NMR study of monomethylamine adsorbed on HY. *Journal of Physical Chemistry*, 100, 5105–5117.
- Kingery, W.D., Bowen, H.K., and Uhlmann, D.R. (1976) *Introduction to Ceramics*. 104–105 p. John Wiley and Sons, Inc.
- Kohn, S.C., Dupree, R., and Smith, M.E. (1989) A multinuclear magnetic-resonance study of the structure of hydrous albite glasses. *Geochimica et Cosmochimica Acta*, 53, 2925–2935.
- Kohn, S.C., Smith, M.E., Dirken, P.J., van Eck, E.R.H., Kentgens, A.P.M., and Dupree, R. (1998) Sodium environments in dry and hydrous albite glasses: Improved Na-23 solid state NMR data and their implications for water dissolution mechanisms. *Geochimica et Cosmochimica Acta*, 62, 79–87.
- Kummerlen, J., Merwin, L.H., Sebald, A., and Keppeler, H. (1992) Structural role of H₂O in sodium-silicate glasses—results from Si-29 and H-1-NMR spectroscopy. *Journal of Physical Chemistry*, 96, 6405–6410.
- Maciel, G.E. and Ellis, P.D. (1994) NMR characterization of silica and alumina surfaces. In A. Pines, Ed., *NMR Techniques in Catalysis*, p. 231. Marcel Dekker, Inc., New York, NY.
- McManus, J., Ashbrook, S.E., MacKenzie, K.J.D., and Wimperis, S. (2001) Al-27 multiple-quantum MAS and Al-27{H-1} CPMAS NMR study of amorphous aluminosilicates. *Journal of Non-Crystalline Solids*, 282, 278–290.
- Mellott, N.P., Brantley, S.L., and Pantano, C.G. (2002) Topography of polished plates of albite crystal and glass during dissolution, in Water-Rock Interactions, Ore Deposits, and Environmental Geochemistry: A Tribute to David A. Crerar. The Geochemical Society, Special Public 7, 83–95.
- Nugent, M.A., Brantley, S.L., Pantano, C.G., and Maurice, P.A. (1998) The influence of natural mineral coatings on feldspar weathering. *Nature*, 395, 588–591.
- Oelkers, E.H. and Schott, J. (1995) Experimental study of anorthite dissolution and the relative mechanism of feldspar hydrolysis. *Geochimica et Cosmochimica Acta*, 59, 5039–5053.
- Oelkers, E.H., Schott, J., and Devidal, J.L. (1994) The effect of aluminum, pH, and chemical affinity on the rates of aluminosilicate dissolution reactions. *Geochimica et Cosmochimica Acta*, 58, 2011–2024.
- Oglesby, J.V. and Stebbins, J.F. (2000) Si-29 CPMAS NMR investigations of silanol-group minerals and hydrous aluminosilicate glasses. *American Mineralogist*, 85, 722–731.
- Onorato, P.I.K., Aleksander, M.N., Struck, C.W., and Tasker, G.W. (1985) Bridging and nonbridging oxygen atoms in alkali aluminosilicate glasses. *Journal of the American Ceramic Society*, 68, C148–C150.
- Pines, A., Gibby, M.G., and Waugh, J.S. (1973) Proton-enhanced NMR of dilute spins in solids. *The Journal of Chemical Physics*, 59, 569–589.
- Riemer, T., Schmidt, B., Behrens, H., and Dupree, R. (2000) H₂O/OH ratio determination in hydrous aluminosilicate glasses by static proton NMR and the effect of chemical shift anisotropy. *Solid State Nuclear Magnetic Resonance*, 15, 201–207.
- Shelby, J.E. (1978) Viscosity and thermal expansion of lithium-aluminosilicate glasses. *Journal of Applied Physics*, 49, 5885–5891.
- Sindorf, D.W. and Maciel, G.E. (1983) Silicon-29 nuclear magnetic resonance study of hydroxyl sites on dehydrated silica gel surfaces, using silylation as a probe. *Journal of Physical Chemistry*, 87, 5516–5521.
- Stebbins, J.F. and Xu, Z. (1997) NMR evidence for excess non-bridging oxygen in an aluminosilicate glass. *Nature*, 390, 60–62.
- Stebbins, J.F., Lee, S.K., and Oglesby, J.V. (1999) Al-O-Al oxygen sites in crystalline aluminates and aluminosilicate glasses: High-resolution oxygen-17 NMR results. *American Mineralogist*, 84, 983–986.
- Stejskal, E.O., Schaefer, J., and Waugh, J.S. (1977) Magic-angle spinning and polarization transfer in proton-enhanced NMR. *Journal of Magnetic Resonance*, 28, 105–112.
- Stillings, L.L. and Brantley, S.L. (1995) Feldspar dissolution at 25-degrees-C and pH 3—reaction stoichiometry and the effect of cations. *Geochimica et Cosmochimica Acta*, 59, 1483–1496.
- Taylor, M. and Brown, G.E. (1979) Structure of mineral glasses—I. The feldspar glasses NaAlSi₃O₈, KAlSi₃O₈, CaAl₂Si₂O₈. *Geochimica et Cosmochimica Acta*, 43, 61–75.
- Vega, A.J. (1992) MAS NMR spin locking of half-integer quadrupolar nuclei. *Journal of Magnetic Resonance*, 96, 50–68.
- Walther, J.V. (1996) Relation between rates of aluminosilicate mineral dissolution, pH, temperature, and surface charge. *American Journal of Science*, 296, 693–728.
- (1997) Comment: Feldspar dissolution at 25 °C and low pH. *American Journal of Science*, 297, 1012–1021.
- Xu, Z., Maekawa, H., Oglesby, J.V., and Stebbins, J.F. (1998) Oxygen speciation in hydrous silicate glasses: An oxygen-17 NMR study. *Journal of the American Chemical Society*, 120, 9894–9901.
- Yang, W.H.A. and Kirkpatrick, R.J. (1989) Hydrothermal reaction of albite and a sodium aluminosilicate glass—a solid-state NMR-study. *Geochimica et Cosmochimica Acta*, 53, 805–819.
- Zavel'sky, V.O., Bezman, N.I., and Zharikov, V.A. (1988) Water in albite glasses: OH-groups, isolated molecules, and clusters. *Journal of Non-Crystalline Solids*, 224, 225–231.
- Zeng, Q., Nekvasil, H., and Grey, C.P. (1999) Proton environments in hydrous aluminosilicate glasses: AH-1 MAS, H-1/Al-27, and H-1/Na-23 TRAPDOR NMR study. *Journal of Physical Chemistry B*, 103, 7406–7415.
- (2000) In support of a depolymerization model for water in sodium aluminosilicate glasses: Information from NMR spectroscopy. *Geochimica et Cosmochimica Acta*, 64, 883–896.
- Zotov, N. and Keppeler, H. (1998) The influence of water on the structure of hydrous sodium tetrasilicate glasses. *American Mineralogist*, 83, 823–834.